Functional Role of the Active Site Glutamate-368 in Rat Short Chain Acyl-CoA Dehydrogenase[†]

Kevin P. Battaile,[‡,§] Al-Walid A. Mohsen,[||] and Jerry Vockley*,[‡,||]

Department of Medical Genetics and Department of Biochemistry and Molecular Biology, Mayo Clinic and Mayo Foundation, Rochester, Minnesota 55905

Received May 10, 1996; Revised Manuscript Received October 8, 1996[⊗]

ABSTRACT: The acyl-CoA dehydrogenases are a family of flavoenzymes with similar structure and function involved in the metabolism of fatty acids and branched chain amino acids. The degree of overlap in substrate specificity is narrow among these enzymes. The position of the catalytic glutamate, identified as Glu376 in porcine medium chain acyl-CoA dehydrogenase (MCAD), Glu254 in human isovaleryl-CoA dehydrogenase (IVD), and Glu261 in human long chain acyl-CoA dehydrogenase (LCAD), has been suggested to affect substrate chain length specificity. In this study, *in vitro* site-directed mutagenesis was used to investigate the effect of changing the position of the catalytic carboxylate on substrate specificity in short chain acyl-CoA dehydrogenase (SCAD). Glu368, the hypothetical active site catalytic residue of rat SCAD, was replaced with Asp, Gly, Gln, Arg, and Lys and the wild type and mutant SCADs were produced in *Escherichia coli* and purified. The recombinant wild type SCAD k_{cat}/K_m values for butyryl-, hexanoyl-, and octanoyl-CoA were 220, 22, and 3.2 μM^{-1} min^{-1}, respectively, while the Glu368Asp mutant gave k_{cat}/K_m of 81, 12, and 1.4 μM^{-1} min^{-1}, respectively, for the same substrates. None of the other mutants exhibited enzyme activity. A Glu368Gly/Gly247Glu double mutant enzyme, which places the catalytic residue at a position homologous to that of LCAD, was also synthesized and purified. It showed k_{cat}/K_m of 9.3, 2.8, and 1.5 μM^{-1} min^{-1} with butyryl-, hexanoyl-, and octanoyl-CoA used as substrates, respectively. These results confirm the identity of Glu368 as the catalytic residue of rat SCAD and suggest that alteration of the position of the catalytic carboxylate can modify substrate specificity.

The acyl-CoA dehydrogenases (ACDs)[1] are a family of flavoenzymes which include short chain acyl-CoA dehydrogenase (SCAD), medium chain acyl-CoA dehydrogenase (MCAD), long chain acyl-CoA dehydrogenase (LCAD), short/branched chain acyl-CoA dehydrogenase (SBCAD), and isovaleryl-CoA dehydrogenase (IVD). All of these enzymes catalyze the α,β-dehydrogenation of their corresponding acyl-CoA substrates. The first three enzymes are involved in the degradation of fatty acids, while SBCAD and IVD are involved in the isoleucine/valine and leucine degradation pathways, respectively (Ikeda et al., 1983, 1985a; Finocchiaro et al., 1987; Matsubara et al., 1989; Rozen et al., 1994; Willard et al., 1996). While these ACDs are thought to have evolved from a common ancestral gene and share significant structural and biochemical similarities, each enzyme can be distinguished by a characteristic substrate specificity profile (Ikeda & Tanaka, 1983a,b; Ikeda et al., 1985a; Willard et al., 1996). X-ray diffraction crystallography has provided data identifying residues involved in substrate binding. The three-dimensional structures of porcine MCAD and butyryl-CoA dehydrogenase (a homologous enzyme from *Megasphaera elsdenii*) have been determined with and without substrate (Kim & Wu, 1988; Kim et al., 1993, 1994; Djordjevic et al., 1995). One structural feature suggested to affect substrate length specificity is the position of the active site catalytic glutamate, which has been identified at two different locations within the active sites of ACDs. An MCAD Glu376Gly/Thr255Glu double mutant enzyme, where the catalytic glutamate has been moved to a location equivalent to that in LCAD, was reported to be more active toward longer chain acyl-CoA substrates compared to the wild type enzyme (Nandy et al., 1996). Similarly, Mohsen and Vockley (1995) reported that the decrease of IVD enzyme activity following placement of the active site catalytic residue of IVD at the equivalent position as in MCAD was significantly less for hexanoyl-CoA than for isovaleryl-CoA.

Covalent modification of the pig SCAD glutamate equivalent to human or rat SCAD Glu368 with 2-pentynoyl-CoA (Lundberg & Thorpe, 1993) and preliminary crystal structure data (Kim et al., 1994) have suggested that Glu368 is the active site catalytic residue in SCAD. In this study, site-directed mutagenesis was used to confirm the identity of rat SCAD Glu368 as the catalytic residue and to monitor the effect of altering the position of the catalytic carboxylate on enzyme kinetics and the spectrophotometric behavior of the enzyme mutants in the presence of substrate.

[†] This work was supported in part by National Institutes of Health Grant RO1-DK45482.

* Author to whom correspondence should be addressed.

[‡] Department of Biochemistry and Molecular Biology.

[§] Present address: Oregon Health Science University, Molecular and Medical Genetics, L103, 3181 Sam Jackson Park Rd., Portland, OR 97201.

[||] Department of Medical Genetics.

[⊗] Abstract published in *Advance ACS Abstracts,* November 15, 1996.

[1] Abbreviations: ACD, acyl-CoA dehydrogenase; DCIP, dichlorophenylindolphenol; CoA, coenzyme A; ETF, electron transferring flavoprotein; FAD, flavin adenine dinucleotide; IPTG, isopropyl-β-D-thiogalactoside; IVD, isovaleryl-CoA dehydrogenase; LCAD, long chain acyl-CoA dehydrogenase; MCAD, medium chain acyl-CoA dehydrogenase; PMS, phenazine methosulfate; SCAD, short chain acyl-CoA dehydrogenase.

S0006-2960(96)01113-0 CCC: $12.00

MATERIALS AND METHODS

Growth of Uracil-Containing Phagemids for in Vitro Mutagenesis. This was performed as described with minor modification (Sambrook et al., 1989). The phagemid pBluescript II SK+ (Stratagene; La Jolla, CA) containing the coding sequence for the mature rat short chain acyl-CoA dehydrogenase was transformed into the *dut*$^-$*ung*$^-$ *Escherichia coli* strain CJ236 (Invitrogen; San Diego, CA) and maintained on LB agar with 30 μg/mL chloramphenicol. Helper phage MK1307 (New England Biolabs; Beverly, MA) was used to produce a phagemid with uracil-containing DNA. Phage were harvested *via* polyethyleneglycol precipitation, and the single-stranded phage DNA was isolated by phenol: chloroform extraction. Isolated DNA was precipitated with ethanol, and the DNA pellet was resuspended in 20 μL of 10 mM Tris, 1 mM EDTA, pH 7.4.

Construction of Rat SCAD Expression Vector. Expression vectors were generated by a PCR-based method from previously cloned cDNA (Matsubara et al., 1989). The 5′ PCR primer contained a translation initiation codon followed by the first 20 nucleotides of the mature SCAD coding sequence. An *Eco*RI restriction site was included upstream of the ATG to facilitate subsequent cloning of the PCR fragment. The 3′ PCR primer consisted of the last 20 nucleotides of the coding sequence including the termination codon followed by a *Hin*dIII restriction site sequence.

M13 Mediated in Vitro Site-Directed Mutagenesis. To verify the importance of the hypothetical catalytic residue for SCAD enzyme activity, site specific mutagenesis was used to replace Glu368 with other amino acids. Site-directed mutagenesis was performed as described (Kunkel, 1985; Kunkel et al., 1987). Mutagenic primers were synthesized by the Mayo Clinic Molecular Biology Core Facility. Primer sequences were as follows: E368G, GAGATCTATGGTGGTACCAGC; E368R, GAGATCTATAGAGGTACCAGC; E368K, GAGATCTATAAGGGTACCAGC; E368Q, GAGATCTATCAGGGTACCAGC; E368D, GAGATCTATGACGGTACCAGC; G247E, CTGGACATGGAACGCATTGGC; D245P, ATAGCCATGCAAACCCTGCCAATGGGCCGCATTGGCATC; I249P, ATACTGGACATGGGCCGCCCAGGCATCGCCTCCCAGGCCCTG.

DNA Sequencing. The sequences of all mutant inserts were confirmed using a 7-deaza-dGTP Sequenase V2.0 kit (Amersham; Arlington Heights, IL) according to the manufacturers instructions. Bands of radioactivity were visualized by overnight exposure to Kodak BioMax (Rochester, NY) or other equivalent film.

Purification of Recombinant SCAD and Mutants. All expression of recombinant enzymes was performed using the IPTG inducible vector pKK223-3 (Pharmacia; Uppsala, Sweden) in *E. coli* strain XL1-Blue or a derivative thereof (Stratagene; La Jolla, CA). Four flasks containing 2 L of LB with 80 μg/mL of ampicillin were inoculated with starter culture and incubated at 37 °C with shaking until absorbance at 600 nm was ~1.2. IPTG was added to a final concentration of 1 mM, and the cultures were incubated overnight at 37 °C with shaking. The cells were then collected by centrifugation, treated with 1 mg/mL lysozyme, and sonicated (Fisher Scientific; Pittsburgh, PA) at high power at least three times for 45 s. Cell debris was removed by centrifugation, and 1 g of pre-swelled DE52 resin (Whatman; Fairfield, NJ) per gram of pre-sonicated cells was added to the supernatant. After incubation for 30 min at 4 °C with gentle agitation, the resin was washed in a Buchner funnel with 25 mM triethylamine, pH 7.6, and then packed into a Pharmacia XK 16/40 column. SCAD was eluted with a 0−400 mM NaCl gradient in 25 mM triethylamine, pH 7.6, over five column volumes. Fractions containing SCAD activity were identified using the DCIP dye reduction assay, and the peak fractions were pooled. The pooled fraction was then chemically reduced by transferring the sample to a side-arm flask and applying 5 cycles of vacuum alternating with purging with dry, oxygen free argon. Following the final argon purge, 10−20 mg of sodium dithionite was added to the flask and the sealed flask was incubated at room temperature for 45 min. The sample was dialyzed overnight at 4 °C against 5 mM potassium phosphate, pH 7.4, applied to a 10 μm ceramic hydroxyapatite matrix column (Bio-Rad; Hercules, CA), and eluted with a 5−500 mM potassium phosphate, pH 7.4, gradient. Fractions containing SCAD were pooled, dialyzed overnight against 25 mM triethylamine, pH 7.6, applied to a Pharmacia Sepharose S Fast Flow column (XK 16/40), and eluted with a 0−1.0 M NaCl gradient of 125 mL. The final peak fractions were pooled and dialyzed against 25 mM Tris, pH 7.5, 20% glycerol for storage at −20 °C. Concentration of proteins was determined using the DC protein assay system from Bio-Rad according to the manufacturers instructions. Flavin content was estimated spectrally using the reported molar extinction coefficient for FAD $\epsilon_{450} = 11.3$ mM^{-1} cm^{-1} (Whitby, 1953).

Enzyme Assays. The DCIP reduction assay was performed as described (Hall, 1978; Mohsen & Vockley, 1995). The ETF reduction assay was performed using an LS50B fluorescence spectrophotometer from Perkin Elmer (Norwalk, CT) with a heated cuvette block set to 32 °C as described (Beckmann et al., 1981; Mohsen & Vockley, 1995). For kinetic analysis, ETF concentration was 1 μM and substrate concentration was varied from 1 to 50 μM final concentration and k_m and V_{max} were calculated on a Macintosh computer using the *EnzymeKinetics v 1.4.1* software from Trinity Software (Campton, NH).

Monitoring the Formation of the Charge Transfer Complex. Formation of the charge transfer complex was monitored as described (Ikeda et al., 1985b). Spectral scans were performed using a DU7400 spectrophotometer from Beckman (Palo Alto, CA) equipped with a computer and a heating block. To a quartz cuvette were added the following: SCAD protein, calculated to give a concentration of approximately 2 nM of FAD, in 500 μL of 10 mM potassium phosphate, 0.1 mM EDTA, 10% glycerol, pH 8.0. Increasing amounts of substrate were then added to the sample in the cuvette and spectral scans were performed after each addition. Substrate concentrations used were 0.912, 1.81, 2.69, 3.55, 4.21, 17.2, 34.1, and 50.0 μM. Scans were performed under aerobic and anaerobic conditions with essentially identical results over the time frame of these experiments. Data from the scans were exported to a personal computer for further analysis. Absorption values at 450 nm as a function of substrate concentrations were plotted using the program *Grafit* from Erithacus Software Ltd. (Staines, U. K.). The values of K_f (where K_f is the substrate concentration which induces half the maximum quenching of the absorbance at 450 nm) and Δ_{max}, a measure of the maximum decrease in absorbance at 450 nm, were then calculated using a nonlinear regression algorithm.

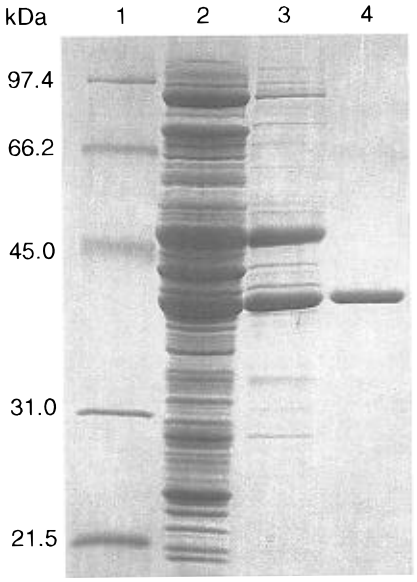

FIGURE 1: Purification of recombinant SCAD. Recombinant SCAD was purified from bacterial extracts as described in text and SDS−PAGE was performed on protein samples after each column step. 5−10 μg of SCAD was loaded in each lane, and the gel was stained with Coomassie blue. Lane 1, Molecular markers from top, phosphorylase B, serum albumin, ovalbumin, carbonic anhydrase, and trypsin inhibitor; lane 2, pooled DE52 peak fractions; lane 3, pooled Matrix Gel Blue A peak fractions; lane 4, pooled Sepharose S peak fractions.

Western Blotting. For Western blotting, proteins were separated by SDS−PAGE (Laemmli, 1970) and the gel transferred to PVDF membrane (Schleicher & Schuell; Keene, NH) using a TE70 SemiPhor apparatus (Hoefer; San Francisco, CA). After transfer, the membrane was treated as described (Willard et al., 1996).

Molecular Modeling of SCAD. Computer modeling of the various wild type and mutant ACDs was performed using a Silicon Graphics workstation and the *Insight II* software package from Molecular Simulations, Inc. (San Diego, CA). With the *Homology* module of the *Insight II* software, the atomic coordinates of butyryl-CoA dehydrogenase were retrieved from the National Center for Biotechnology Information (Bethesda, MD) and used to assign coordinates for the SCAD atomic structure. Replacements of SCAD Glu368 and Gly247 were modeled into a hypothetical SCAD model, and the *Discover* module was used to minimize energy and draw the best possible three-dimensional model for SCAD mutants.

RESULTS

Purification of Rat SCAD from E. coli. Purification of SCAD from 4 L of induced bacterial cultures yielded approximately 0.8 mg of SCAD per gram of wet bacterial paste. Only the SCAD protein band was visible with the SDS−PAGE (Figure 1); a sample of this recombinant SCAD preparation was crystallized for three-dimensional structure determination and preliminary results have been reported (Kim et al., 1994). To enhance the stability of the mutant enzymes during purification, 10% ethylene glycol and 0.1 mM FAD were added to all buffers. Using the molar extinction coefficient of FAD, the FAD content of the purified wild type recombinant rat SCAD was calculated to be, on average, greater than three moles of FAD per mole of enzyme (Table 1). Glu368Gly and Glu368Gln were only partially purified for further spectrophotometric analysis (90−95% purity as judged by SDS−PAGE, data not shown).

Table 1: FAD Content and Absorption Maxima of Wild Type and Mutant SCAD.

enzyme	271:365:450 ratio	FAD:tetramer ratio	specific activity[a]
wild type	6.60:0.81:1	3.5:1	3.8[b]
E368G/G247E	7.88:0.71:1	2.4:1	0.3[c]
E368D	8.82:0.74:1	2.8:1	1.9[c]
E368Q	11.1:0.68:1	3.9:1	ND[d]
E368G	5.96:0.71:1	4.0:1	ND[d]

[a] In μmol of ETF reduced min^{-1} (mg of enzyme)$^{-1}$. [b] Determined with 20 μM butyryl-CoA as substrate. [c] Determined with 50 μM butyryl-CoA as substrate. [d] No detectable activity.

Spectral Analysis. The absorption spectra of the wild type recombinant SCAD without substrate present did not differ significantly from that previously reported for SCAD purified from rat liver (Figure 2; Ikeda et al., 1985b). All of the recombinant enzymes show absorption maxima near 270, 370, and 450 nm characteristic of the spectrum of FAD. With the exception of Glu368Gln, they also exhibit a shoulder at approximately 279 nm. The absolute placement of these maxima varies among the various enzymes. Upon titration of substrate into a solution of enzyme, the 270 nm peak could not be distinguished for all of the wild type enzyme and mutants because of the appearance of an absorption maximum at 261 nm, which corresponds to the absorption maxima of the adenine of the CoA moiety of the substrate.

(1) Wild Type SCAD. The spectral data provide evidence for the formation of the charge transfer complex upon addition of substrate to the enzyme solution (Thorpe et al., 1979; Figure 2). The intermediate, ACD·FAD$_{2e}$ + product, binary complex appears kinetically stable in the absence of an electron acceptor, as is evident from the stability of these scans with time. In this state the complex exhibits the characteristic quenching of absorption at 450 nm and appearance of a new absorption band at $\lambda \approx 580$ nm (Ikeda et al., 1985b). Titrating butyryl- or hexanoyl-CoA into wild type enzyme results in a blue-shift of the 370 nm peak by 15−20 nm and minor shifts of up to 5 nm in the 450 nm peak. Titration of wild type enzyme with octanoyl-CoA results in a 5 nm similar shift of the 370 nm peak and a 10 nm red-shift of the 450 nm-peak. Changes seen with the addition of palmitoyl-CoA include an absorption maximum at 470 nm as well as shoulders at approximately 497 and 442 nm. Additionally, the usual 370 nm peak is replaced by absorbance maxima at 362 and 377 nm.

(2) SCAD Mutants. The SCAD Glu368Gly and Glu368Gln mutants UV−visible spectra were found to be similar to the native enzyme. The SCAD Glu368Gly mutant had an additional shoulder at 475 nm. Titration of the Glu368Gly mutant with butyryl-, hexanoyl-, and octanoyl-CoA results in a red-shift of the 370 nm peak to 378 nm and a slight red-shift of the 450 nm peak. Titration of the Glu368Asp mutant with butyryl-CoA results in a 10 nm blue-shift of the 370 nm peak and minor inconsistent shifts in the 450 nm peak tending toward longer wavelength. Adding hexanoyl- or octanoyl-CoA to the Glu368Asp enzyme results in changes in the shape of the spectrum around 370 and 450 nm with no obvious alteration in absorption maxima. Titration of Glu368Gln with butyryl-CoA results in a 11 nm red-shift of the 364 nm peak with no significant change in

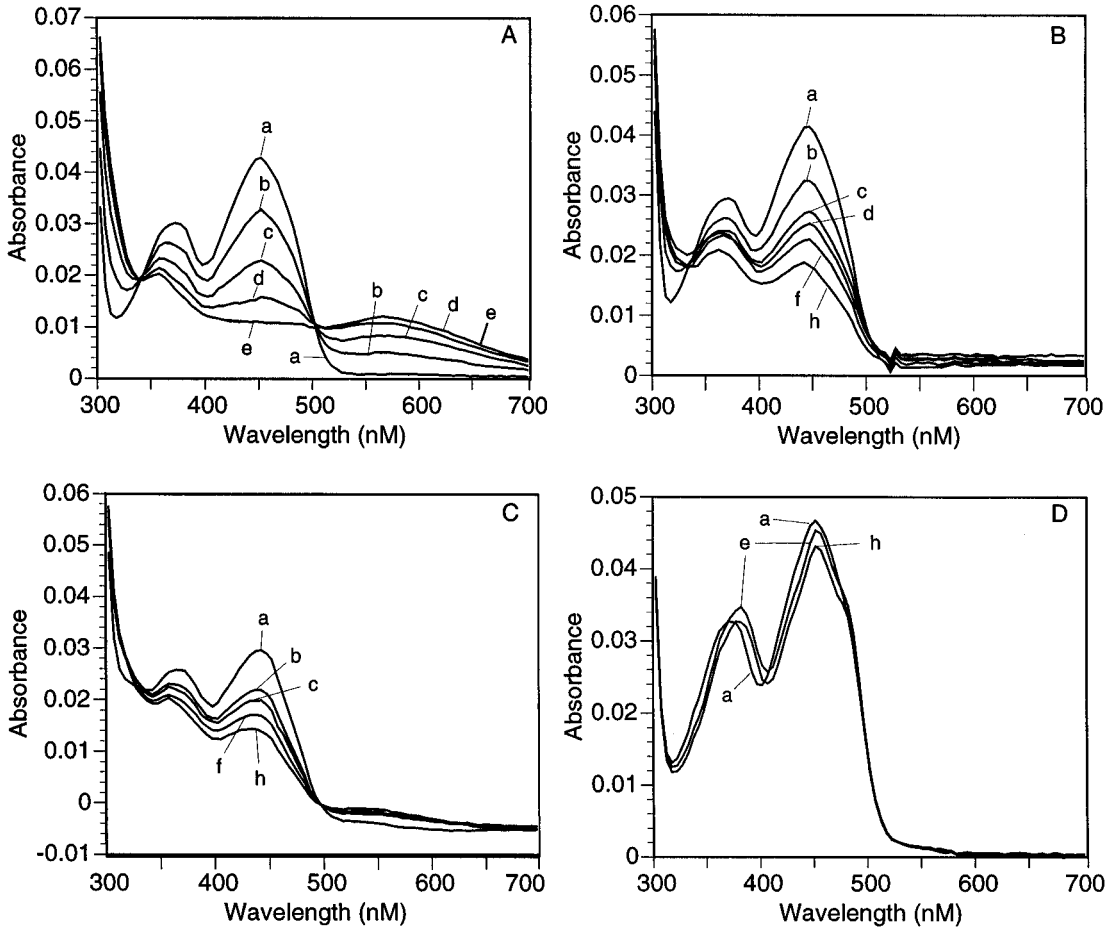

FIGURE 2: Comparison of absorbance spectra of wild type and mutant SCADs titrated with butyryl-CoA. Increasing concentrations of butyryl-CoA were added to purified enzymes, and then the absorbance was read from 250 to 700 nm. (A) Wild type recombinant SCAD. (B) Glu368Asp. (C) Glu368Gly/Gly247Glu. (D) Glu368Gly. Butyryl-CoA concentrations used were as follows: (A) a, 0, 0.919 μM; b, 1.84 μM; c, 2.75 μM; d, 3.67 μM; e, 4.58 μM. (B−D) a, 0, 0.912 μM; d, 1.81 μM; b, 2.69 μM; c, 3.55 μM; d, 4.21 μM; e, 17.2 μM; f, 34.1 μM; g, 50.0 μM. Curves for some substrate concentrations are not shown for the sake of clarity.

absorbance. The 446 nm peak shows minor shifts with higher substrate concentrations. Titration of the Glu368Gln enzyme with hexanoyl- and octanoyl-CoA results in minor fluctuations of the 364 and 442 nm maxima. Titration of the Glu368Gly/Gly247Glu enzyme with butyryl-, hexanoyl-, and octanoyl-CoA all result in fluctuations around the absorption maxima, but butyryl- and hexanoyl-CoA appear to shift the 364 nm peaks to 354 nm. None of the SCAD enzymes, including the wild type, shows substantial changes in absorbance with palmitoyl-CoA titration.

Flavin absorption spectra were monitored at various substrate concentrations, and the values K_f (the substrate concentration which induces half the maximum quenching of the absorbance at 450 nm), and Δ_{max} (a measure of the maximum decrease in absorbance at 450 nm) were then calculated. In these experiments, all of the SCAD enzymes demonstrate the highest Δ_{max} toward butyryl-CoA and the least toward octanoyl-CoA with no demonstrable productive association with palmitoyl-CoA (Table 3). Wild type SCAD shows the largest change in Δ_{max} between butyryl-CoA and octanoyl-CoA. This change is less pronounced in the Glu368Asp mutant and less still for the Glu368Gly/Gly247Glu mutant. The change in the K_f also shows a similar change relative to substrate chain length, with the mutant enzymes having a lower magnitude of change with increasing substrate length compared to the wild type SCAD. No change in absorbance was observed with addition of substrate to any of the inactive mutants.

Enzyme Activity of SCAD in Crude Lysates. cDNAs encoding the SCAD amino acid sequence and harboring the desired mutations were cloned into the pKK223-3 vector and transformed into *E. coli*, and the inserts were expressed as described for native SCAD. Crude lysates from the Glu368Gly, Gln, Lys, and Arg mutants showed no detectable activity with the ETF fluorescence reduction assay using either butyryl-, hexanoyl-, octanoyl-, isobutyryl-, isovaleryl-, 2-methylbutyryl-, or palmitoyl-CoA as substrate. In contrast, lysates for the Glu368Asp, and Glu368Gly/Gly247Glu mutants showed activity with several substrates and both enzymes were purified for further analysis (Table 1).

Enzyme Activity of Purified Wild Type and Mutant SCADs. Purification of the wild type and mutant SCADs were monitored with SDS−PAGE and western blotting. Catalytic activity of SCAD wild type and mutants was monitored using the anaerobic ETF fluorescence reduction assay and kinetic parameters were calculated using the *Enzyme Kinetics* software package. The production of inactive mutants was monitored by western blotting. Partially purified SCAD Glu368Gly, Glu368Gln, and Glu368Lys mutants had no enzyme activity. Kinetic data for active wild type and mutant SCADs are shown in Table 2. The recombinant wild type enzyme has the highest V_{max} with butyryl-CoA as substrate and decreases with hexanoyl-CoA and octanoyl-CoA as substrate. The K_m and k_{cat}/K_m also show increases and

Table 2: Kinetic Parameters of the Recombinant Wild Type SCAD and Functional Mutants

substrate	kinetic parameter	enzyme: SCAD	enzyme: Glu368Asp	enzyme: Glu368Gly/ Gly247Glu
butyryl-CoA	V_{max}[a]	2.8	2.0	0.3
	K_m[b]	0.6	1.5	2.0
	k_{cat}/K_m[c]	220	81	9.3
hexanoyl-CoA	V_{max}[a]	1.8	1.0	0.07
	K_m[b]	3.8	5.0	1.7
	k_{cat}/K_m[c]	22	12	2.8
octanoyl-CoA	V_{max}[a]	0.52	0.1	0.02
	K_m[b]	8.1	5.0	1.1
	k_{cat}/K_m[c]	3.2	1.4	1.5

[a] In s^{-1} as computed from the values of μmole of ETF reduced min^{-1} (mg of enzyme)$^{-1}$. [b] In μM. [c] In (μM of ETF reduced)$^{-1}$ (μM of FAD)$^{-1}$ min^{-1}.

Table 3: Kinetic Parameters of Flavin Reduction of the Recombinant and Wild Type and Mutant SCADs by Various Acyl-CoAs

substrate	kinetic parameter	enzyme: SCAD	enzyme: Glu368Asp	enzyme: Glu368Gly/ Gly247Glu
butyryl-CoA	Δ_{max}[a]	2.4×10^{-2}	2.3×10^{-2}	1.6×10^{-2}
	K_f[b]	8.2×10^{-1}	2.2	1.5
hexanoyl-CoA	Δ_{max}[a]	1.7×10^{-2}	1.9×10^{-2}	1.4×10^{-2}
	K_f[b]	1.7	5.0	1.5
octanoyl-CoA	Δ_{max}[a]	5.8×10^{-3}	1.0×10^{-2}	1.1×10^{-2}
	K_f[b]	2.1	2.2	3.0

[a] Maximum change in absorbance units at 450 nm. [b] In mM substrate at one-half Δ_{max}.

decreases in value, respectively, with increasing substrate chain length indicating less efficient use of the longer chain substrates. The Glu368Asp mutant enzyme shows a greater decrease in V_{max} with hexanoyl-CoA and octanoyl-CoA as substrates than does the wild type enzyme. The pattern of change of K_m and k_{cat}/K_m is similar to wild type SCAD; however, the magnitude of change in both parameters between butyryl-CoA and octanoyl-CoA is slightly lower compared to the wild type enzyme. The Glu368Gly/ Gly247Glu mutant also has the greatest V_{max} with butyryl-CoA as substrate, which then decreases with longer chain substrates. In contrast to the wild type enzyme and Glu368Asp mutant, the Glu368Gly/Gly247Glu mutant shows the highest K_m with butyryl-CoA, which then decreases with increasing substrate chain length. The magnitude of the change of the k_{cat}/K_m with butyryl- and octanoyl-CoA as substrates is also less than seen with the Glu368Asp enzyme. Similar findings were obtained using PMS and DCIP as intermediate and final electron acceptors, respectively (data not shown). None of the enzymes demonstrated activity against palmitoyl-CoA.

Molecular Modeling. Preliminary X-ray crystallography data for rat SCAD have indicated that its three-dimensional structure reasonably match that of butyryl-CoA dehydrogenase (Kim et al., 1994; J. J. P. Kim, personal communication). To provide some insights on the structural differences between SCAD and MCAD active sites and to evaluate our site-directed mutagenesis experiments with a hypothetical molecular model, the three-dimensional structure of butyryl-CoA dehydrogenase with bound acetoacetyl-CoA was used as the reference structure of substrate-bound SCAD and was then compared to that of MCAD with bound octanoyl-CoA (Kim et al., 1993; Djordjevic et al., 1995). According to the published atomic coordinates of MCAD and butyryl-CoA dehydrogenase crystals, the peptide backbone of the catalytic residue in MCAD would be estimated to lie 0.5 Å farther and its carboxylate 1.5 Å farther from the substrate than in rat SCAD. In SCAD, the distance from the γ-carbon of Glu368 to the α-carbon of the substrate would be 3.57 Å, while it would be 3.46 Å from the substrate β-carbon to the N-5 position of the FAD. In MCAD, the distance between the catalytic residue γ-carbon and the substrate α-carbon is 4.33 Å. The distance from the SCAD catalytic residue α-carbon to the substrate α-carbon would be 4.16 Å and 7.02 Å from the Gly247 α-carbon (LCAD catalytic residue position) while in MCAD this distance is 8.89 Å (Figure 3). The distance between the SCAD and MCAD α-carbons at the LCAD/IVD catalytic residue location is 1.95 Å due to a trajectory difference in the G-helix. The angle between the SCAD catalytic residue α-carbon and the α-carbon of Gly247 with the α-carbon of the substrate as vertex is nearly 72° (Figure 3). Replacing the catalytic glutamate in SCAD with an aspartate reduces the residue side chain length from 3.81 Å to approximately 2.63 Å and the distance to the substrate to approximately 3.17 Å. Modeling a glutamate in position 247 predicts a distance from the γ-carbon of the glutamate to the α-carbon of the substrate of approximately 3.5 Å in SCAD and 6.0 Å in MCAD (Figure 3).

X-ray crystal structure and computer modeling of the binding pocket of the ACDs has also identified differences in the trajectory of the G-helix that may play a role in determining substrate specificity [Kim et al. (1994) and see Figure 3]. One notable difference is the presence of a proline in the G-helix of LCAD at position 245 and in MCAD at position 249 (SCAD numbering), while no prolines exist near these locations in the SCAD. The presence of these prolines has been reported to introduce a sharp bend in the G-helix in MCAD and hypothesized to do the same in LCAD allowing for enhanced binding of longer chain substrates (Kim et al., 1994). Accordingly, SCAD mutants were created to introduce prolines at positions 245 and 249 singly or in conjunction with the double mutant E368G/G247E and expressed in *E. coli*. Although stable mutant proteins were identified in the cytoplasmic (soluble) fraction of cells containing the plasmid vectors as determined by western blotting, enzyme activity could not be detected with butyryl-, hexanoyl-, octanoyl-, or palmitoyl-CoA used as substrates (data not shown).

DISCUSSION

In the proposed mechanism of the α,β-dehydrogenation reaction catalyzed by ACDs, the acyl-CoA substrate binds to the enzyme forming a charge transfer complex. The formation of the charge transfer complex is initiated with the abstraction of the substrate *pro-R* α-hydrogen as a proton by the active site carboxylate. In the absence of an electron acceptor, namely, ETF, the transfer of the substrate *pro-R* β-hydrogen as a hydride to the N-5 of the FAD is postulated to be incomplete, creating a "resonant donor/acceptor hybrid species" (Ikeda et al., 1985a,b), and the acyl-CoA substrate/ product remains tightly bound to the enzyme. Under physiological conditions, the charge transfer complex interacts with ETF, and the reduced ETF and enoyl-CoA are released as the end products to regenerate the oxidized enzyme (ACD·FAD). The interaction between the substrate

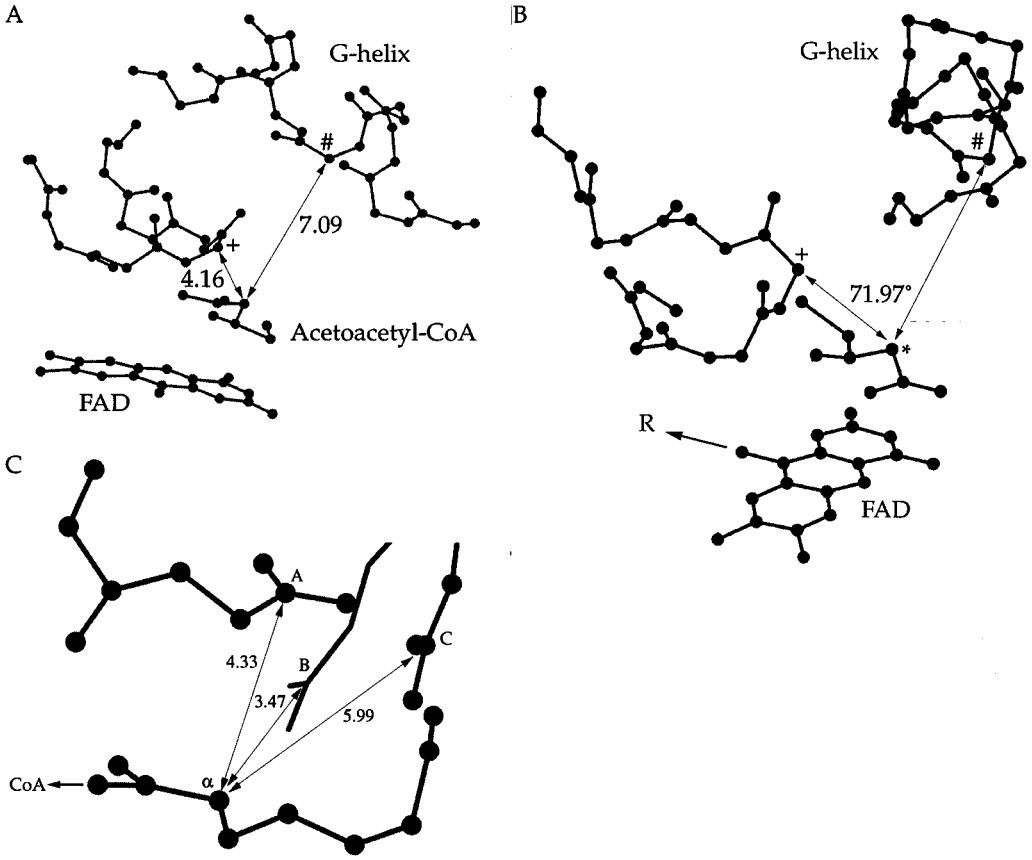

FIGURE 3: Calculated distances between atoms of the catalytic residue of SCAD. (A) The difference in the distance between the α-carbon of the SCAD catalytic residue (+, Glu368) and the α-carbon of the catalytic residue at the LCAD/IVD catalytic residue position (#, Gly247) relative to the α-carbon of acetoacetyl-CoA in the binding pocket is shown. The ball-and-stick trace is of the peptide backbone. (B) The angle measured between the α-carbons of the SCAD catalytic residue (+, Glu368) and the LCAD/IVD catalytic residue position (#, Gly247) is shown with the α-carbon of an acetoacetyl-CoA substrate in the binding pocket as the vertex (*). The ball-and-stick trace is of the peptide backbone with measurement in degrees. (C) Distances from the δ-carbons of the MCAD catalytic residue (A, Glu376) and glutamates substituted into the SCAD (B, Gly247) and MCAD (C, Thr255) positions homologous to the LCAD/IVD catalytic residue position are shown to the α-carbon of octanoyl-CoA. Despite the difference in distance between the α-carbons and angle difference, the δ-carbons of the glutamate in either case are hypothesized to be in roughly the same area. All distances are shown in angstroms and estimated using the *Insight II* software package from Molecular Simulations, Inc.

and the active site base and the oxidized FAD disrupts the extended π-electron system of the FAD isoalloxazine ring, quenching its absorbency at 450 nm and causing a new absorption band to appear at 580 nm (Massey & Ghisla, 1974; Thorpe et al., 1979; Ikeda et al., 1985a, 1985b ; Thorpe, 1991; Thorpe & Kim, 1995). To confirm the identity of the SCAD active site hypothetical catalytic glutamate and to characterize substrate chain length specificity of the recombinant wild type and mutant enzymes, two aspects of enzyme/substrate interactions were investigated: (1) the ability of the SCAD mutants to bind the various substrates individually, which was monitored spectrally and (2) the ability of the active SCAD mutants to transfer electrons from the hypothetical charge transfer complex to ETF, which was monitored using the ETF fluorescence reduction assay.

Identification of the SCAD Active Site Catalytic Residue. The spectral and the ETF fluorescence reduction measurements of the wild type and mutant recombinant rat SCADs confirm the identity of the rat SCAD Glu368 as the catalytic residue. The most obvious changes in these measurements occurred with the SCAD Glu368Gly and Glu368Gln mutants. The similarity of the spectral scans of SCAD wild type and these two mutants suggests that these enzymes had appropriately incorporated FAD and that the replacement of the Glu368 side chain with a hydrogen or its carboxylate with an amide group does not grossly disrupt the FAD isoalloxazine ring. The shifts in absorbance maxima in the spectral scans of the SCAD Glu368Gly and Glu368Gln mutants in the presence of substrate indicate that these two proteins are capable of binding the substrate, consistent with earlier studies with LCAD and IVD (Djordjevic et al., 1994; Mohsen & Vockley, 1995). However, addition of the substrates to these mutants did not induce quenching of absorption at 450 nm, indicating an inability to form the charge transfer complex. This correlates well with the inability of these mutant enzymes to catalyze the α,β-dehydrogenation of the substrate and transfer electrons to the ETF. While these mutants had no detectable activity, the SCAD Glu368Asp mutant and the SCAD Glu368Gly/Gly247Glu had significant activity toward several of the acyl-CoA substrates used, indicating that elimination of a carboxylate base at this position was the primary cause for loss of activity in the other mutants. These results are consistent with findings from sequence homology alignment of rat SCAD and butyryl-CoA dehydrogenase from *M. elsdenii*, preliminary crystal structure of rat SCAD (Kim et al., 1994), and the evidence presented by Lunderberg and Thorpe (1993) who have identified the glutamate involved in the formation of a 2-pentynoyl-CoA·pig SCAD covalent binary complex as the one corresponding to Glu368 of human or rat SCAD.

Substrate Specificity Modification. Conversion of the catalytic glutamate to an aspartate, effectively shortening the catalytic residue side chain by one methylene group, yielded an active SCAD mutant. Kinetic parameters for Glu368Asp were comparable to wild type enzyme using butyryl-CoA as substrate. Both enzymes had lower V_{max} and k_{cat}/K_m values using hexanoyl-CoA as substrate. Both enzymes also showed lower catalytic efficiency with octanoyl-CoA used as substrate; however, in this instance, the decrease in efficiency is slightly less in the mutant enzyme than in the wild type. Similar findings with the DCIP reduction assay support the conclusion that the reduced enzymatic activity of the mutant proteins is not due to a defect in interaction with ETF as an electron acceptor. The flavin reduction data parallel the kinetic data. Wild type SCAD demonstrated lower Δ_{max} and higher K_f as substrate chain length increases from butyryl- to octanoyl-CoA. The Glu368Asp mutant showed a similar trend as the wild type; however, the magnitude of change seen for Δ_{max} and K_f over the substrate range is less. Here, Δ_{max} with butyryl-CoA as substrate was in the range of wild type, but the K_f was twice as large as wild type enzyme. Δ_{max} for hexanoyl-CoA decreased for both enzymes but less so for the Glu368Asp mutant. Both enzymes again showed a decrease in Δ_{max} and K_f with octanoyl-CoA, with less change observed for the Glu368Asp mutant. Notably, the Δ_{max} of the mutant enzyme was double that of the wild type enzyme. Thus the overall trends of Δ_{max} and K_f indicate that the Glu368Asp enzyme has enhanced affinity for binding longer chain substrates as compared to wild type. One potential reason is that the shorter aspartate side chain may allow longer chain substrates greater access to the binding pocket and/or more freedom of motion in the binding pocket than does the glutamate residue.

In the SCAD Glu368Gly/Gly247Glu double mutant where the glutamate has been introduced in a position homologous to that of the catalytic residue of LCAD and IVD, V_{max} was the highest with butyryl-CoA and lowest with octanoyl-CoA. Notably, however, the K_m of the Glu368Gly/Gly247Glu mutant enzyme was lower for octanoyl-CoA compared to butyryl-CoA. The flavin reduction data for this mutant correlated well with the kinetic data. The Δ_{max} of wild type enzyme for octanoyl-CoA decreased to 24% of the butyryl-CoA value whereas this value for the Glu368Gly/Gly247Glu was only 67%. The K_f for octanoyl-CoA increased 2.6 times compared to butyryl-CoA for wild type but only doubled for the Glu368Gly/Gly247Glu enzyme. These data indicate that the binding affinity of the double mutant SCAD is higher for octanoyl-CoA than for the wild type enzyme as compared to butyryl-CoA. Additionally, the magnitude of change in the k_{cat}/K_m when butyryl-CoA and octanoyl-CoA was used as substrate was an order of magnitude less for the Glu368Gly/Gly247Glu mutant than for the wild type enzyme (6.2- *vs* 69-fold). This and the higher binding affinity of the double mutant for octanoyl-CoA imply that the orientation of the catalytic residue in the binding pocket affects substrate specificity. One reason for this may be that moving the catalytic residue across the binding pocket allows more space for longer chain substrates to access an otherwise tight pocket and engage in productive binding. Alternatively, the move may result in changes in conformation that deepen the binding pocket and allow for longer chain substrates to bind.

Two other reports have described altered substrate specificity in similar experiments (Nandy et al., 1996; Mohsen & Vockley, 1995). Moving the catalytic residue in MCAD to the LCAD/IVD position resulted in a mutant enzyme with maximal activity toward lauryl-CoA rather than octanoyl-CoA, as well as in a narrower range in the length of the carbon chain of the acyl-CoA which could be utilized as substrate (Nandy et al., 1994). An IVD double mutant enzyme in which the catalytic residue had been moved to the MCAD/SCAD position exhibited an increased ability to utilize hexanoyl-CoA relative to isovaleryl-CoA as compared to the wild type enzyme (Mohsen & Vockley, 1995). This may be a relatively nonspecific effect of an altered binding pocket being less able to tolerate the bulkier methyl group at the β-carbon of the substrate as compared to straight chain substrate. In combination with our results, this suggests that the binding of long chain substrates is enhanced when the catalytic residue is in the position homologous to that seen in LCAD/IVD.

Molecular Modeling. In the three-dimensional computer model of the SCAD or the MCAD with substrate/product, the $C_\alpha-C_\beta$ axis of the side chain of the catalytic residue, the alkyl chain of the acyl-CoA, and the FAD isoalloxazine ring plane are arranged in parallel, with the rectus face of the isoalloxazine ring at one side facing the alkyl chain of the substrate and the side chain of the catalytic glutamate on the other side of the substrate. In LCAD, the arrangement of the FAD isoalloxazine ring and the alkyl chain of the acyl-CoA substrate is similar to that of SCAD and MCAD. However, the side chain of its active site glutamate approaches the C_α of the substrate from a different direction. The angle between the position of the LCAD active site glutamate, the C_α of the substrate, and the Gly382 position (LCAD Gly382 is the position equivalent to the MCAD Glu376) is almost 80° (Kim el al., 1994). Despite the difference in the oreintation and the position from which the catalytic glutamate side chain approaches the substrate α-carbon in SCAD/MCAD versus LCAD/IVD, the catalytic carboxylate in either case is predicted to occupy similar positions in the active site. Therefore, an interchange of the position of the catalytic residue in any of these ACDs was expected to produce a protein with some enzyme activity. The results presented above are consistent with this prediction and earlier results with MCAD and IVD catalytic residue double mutation experiments (Nandy et al., 1996; Mohsen & Vockley, 1995). Substitution of an aspartate at the LCAD/IVD catalytic residue position would move the active carboxyl group farther away from the α-carbon of the substrate thus significantly reducing its ability to function catalytically. In contrast, the position and orientation of the active site carboxyl group will be less affected with the substitution of an aspartate for a glutamate in the SCAD/MCAD position, compared to the former case, and would be predicted to lead to less drastic effects on catalytic activity. Our findings are in agreement with these predictions and are consistent with earlier findings where substitution of an aspartate for the catalytic glutamate in IVD was reported to lead to an enzyme with less than 0.1% of wild type activity toward isovaleryl-CoA (Mohsen & Vockley, 1995).

Finally, human short/branched-chain acyl-CoA dehydrogenase (SBCAD) is most active in the presence of short-chain substrates with or without a methyl group at the substrate's acyl moiety α-carbon position. The presence of

the catalytic residue of SCAD, MCAD, and SBCAD at the same position (Bross et al., 1990; Ghisla et al., 1992; Kim et al., 1993; Binzak et al., 1995) and results from the catalytic residue double mutation experiments (Nandy et al., 1994; Mohsen & Vockley, 1995; and present study) suggest that the position of the catalytic residue together with other structural aspects, specially those within the active sites, act in concert to determine substrate specificity and provide efficiency for optimum substrate utilization. There are other factors that could affect substrate specificity and enzyme competency. Amino acid residues which are part of the acyl moiety binding site may act directly and/or indirectly by inducing secondary conformational changes following binding of the substrate or affecting the position of other residues to enhance the affinity of the enzyme for one substrate versus another. It has been suggested that a proline residue present in the G-helix bordering the substrate binding pocket in MCAD and LCAD, but not present in SCAD, may lead to a more open conformation of the catalytic site allowing for access of longer chain substrates (Kim et al., 1994). However, enzyme activity could not be detected in *E. coli* cell-free extracts containing SCAD wild type or the catalytic residue double mutant with corresponding proline mutations. The exact cause of loss of activity, however, could result from conformational perturbation(s) at the substrate binding site. Other amino acid residues have been identified which form the substrate's acyl moiety binding pocket using X-ray crystallography (Kim et al., 1993; Djordjevic et al., 1995). These residues and their corresponding counterparts in other ACDs are exciting options for future studies to determine the extent of their involvement in determining substrate binding affinity and specificity.

ACKNOWLEDGMENT

The authors thank Dr. Jung-Ja Kim of the Medical College of Wisconsin for her insightful discussions on the structures of the ACDs and the mechanism of substrate specificity in the ACD enzyme family.

REFERENCES

Beckmann, J. D., Frerman, F. E., & McKean, M. C. (1981) *Biochem. Biophys. Res. Commun. 102*, 1290−1294.

Binzak, B. A., Willard, J., & Vockley, J. (1995) *Am. J. Human Genet. 57 (Suppl.)*, A176.

Bross, P., Engst, S., Strauss, A. W., Kelly, D. P., Rasched, I., & Ghisla, S. (1990) *J. Biol. Chem. 265*, 7116−7119.

Djordjevic, S., Dong, Y., Paschke, R., Frerman, F. E., Strauss, A. W., & Kim, J. J. P. (1994) *Biochemistry 33*, 4258−4264.

Djordjevic, S., Pace, C. P., Stankovich, M. T., & Kim, J. J. P. (1995) *Biochemistry 34*, 2163−2171.

Finocchiaro, G., Ito, M., & Tanaka, K. (1987) *J. Biol. Chem. 262*, 7982−7989.

Frerman, F. E., & Turnbull, D. (1990) in *Fatty Acid Oxidation: Clinical, Biochemical and Molecular Aspects* (Tanaka, K., & Coates, P. M., Eds.) pp 79−89, Alan R. Liss, Inc., New York.

Ghisla, S., Engst, S., Moll, M., Bross, P., Stauss, A. W., & Kim, J.-J. P. (1992) *Prog. Clin. Biol. Res. 375*, 127−142.

Hall, C. L. (1978) *Methods Enzymol. 53*, 502−518.

Ikeda, Y., & Tanaka, K. (1983a) *J. Biol. Chem. 258*, 9477−9487.

Ikeda, Y., & Tanaka, K. (1983b) *J. Biol. Chem. 258*, 1077−1085.

Ikeda, Y., Dabrowski, C., & Tanaka, K. (1983) *J. Biol. Chem. 258*, 1066−1076.

Ikeda, Y., Ikeda, K. O., & Tanaka, K. (1985a) *J. Biol. Chem. 260*, 1311−1325.

Ikeda, Y., Okamura-Ikeda, K., & Tanaka, K. (1985b) *Biochemistry 24*, 7192−7199.

Kim, J.-J., & Wu, J. (1988) *Proc. Natl. Acad. Sci. U.S,A, 84*, 6677−6681.

Kim, J. J. P., Wang, M., & Paschke, R. (1993) *Proc. Natl. Acad. Sci. U.S.A. 90*, 7523−7527.

Kim, J. J. P., Wang, M., Djordjevic, S., Paschke, R., Bennett, D. W., & Vockley, J. (1994) in *Flavins and Flavoproteins 1993* (Yagi, K., Ed.) pp 273−282, Walter de Gruyter, New York.

Kunkel, T. A. (1985) *Proc. Natl. Acad. Sci. U.S.A. 82*, 488−492.

Kunkel, T. A., Roberts, J. D., & Zakour, R. A. (1987) in *Methods in Enzymology* (Wu, R., & Grossman, L., Eds.) pp 367−382, Academic Press, Inc., New York.

Laemmli, U. K. (1970) *Nature 227*, 680−685.

Lundberg, N. N., & Thorpe, C. (1993) *Arch. Biochem. Biophys. 305*, 454−459.

Massey, V., & Ghisla, S. (1974) *Ann. N.Y. Acad. Sci. 227*, 446−455.

Matsubara, Y., Indo, Y., Naito, E., Ozasa, H., Glassberg, R., Vockley, J., Ikeda, Y., Kraus, J., & Tanaka, K. (1989) *J. Biol. Chem. 264*, 16321−16331.

Mohsen, A.-W. A., & Vockley, J. (1995) *Biochemistry 34*, 10146−10152.

Nandy, A., Kieweg, V., Kräutle, F.-G., Vock, P., Küchler, B., Bross, P., Kim, J.-J. P., Rasched, I., & Ghisla, S. (1996) *Biochemistry 35*, 12402−12411.

Rozen, R., Vockley, J., Zhou, L., Milos, R., Willard, J., Fu, K., Vicanek, C., Low-Nang, L., Torban, E., & Fournier, B. (1994) *Genomics 24*, 280−287.

Sambrook, J., Fritsch, E. F., & Maniatis, T. (1989) *Molecular Cloning: A Laboratory Manual*, 2nd ed., Cold Spring Harbor Laboratory Press, Plainview, New York.

Thorpe, C. (1991) in *Chemistry and Biochemistry of Flavoenzymes*, pp 471−486, CRC Press, Inc., Boca Raton, FL.

Thorpe, C., & Kim, J. J. P. (1995) *FASEB J. 9*, 718−725.

Thorpe, C., Matthews, R. G., & Williams, C. H. (1979) *Biochemistry 18*, 331−337.

Whitby, L. G. (1953) *Biochem. J. 54*, 437−442.

Willard, J., Vicanek, C., Battaile, K. P., Van Veldhoven, P. P., Fauq, A. H., Rozen, R., & Vockley, J. (1996) *Arch. Biochem. Biophys. 331*, 127−133.

BI961113R